

1 **Effect of FMRFamide on voltage-dependent currents in identified centrifugal**
2 **neurons of the optic lobe of the cuttlefish, *Sepia officinalis***

3

4 Abdesslam Chrachri

5 University of Plymouth, Dept of Biological Sciences, Drake Circus, Plymouth, PL4

6 8AA, UK and the Marine Biological Association of the UK, Citadel Hill, Plymouth

7 PL1 2PB, UK

8 Phone: 07931150796

9 Email: aacc@mba.ac.uk

10

11 **Running title:** Membrane currents in centrifugal neurons

12

13 **Key words:** cephalopod, voltage-clamp, potassium current, calcium currents, sodium
14 current, FMRFamide.

15

16 Summary: FMRFamide modulate the ionic currents in identified centrifugal neurons
17 in the optic lobe of cuttlefish: thus, FMRFamide could play a key role in visual
18 processing of these animals.

19

20 **Abstract**

21 Whole-cell patch-clamp recordings from identified centrifugal neurons of the optic
22 lobe in a slice preparation allowed the characterization of five voltage-dependent
23 currents; two outward and three inward currents. The outward currents were; the 4-
24 aminopyridine-sensitive transient potassium or A-current (I_A), the TEA-sensitive
25 sustained current or delayed rectifier (I_K). The inward currents were; the tetrodotoxin-
26 sensitive transient current or sodium current (I_{Na}). The second is the cobalt- and
27 cadmium-sensitive sustained current which is enhanced by barium and blocked by the
28 dihydropyridine antagonist, nifedipine suggesting that it could be the L-type calcium
29 current (I_{CaL}). Finally, another transient inward current, also carried by calcium, but
30 unlike the L-type, this current is activated at more negative potentials and resembles
31 the low-voltage-activated or T-type calcium current (I_{CaT}) of other preparations.
32 Application of the neuropeptide FMRFamide caused a significant attenuation to the
33 peak amplitude of both sodium and sustained calcium currents without any apparent
34 effect on the transient calcium current. Furthermore, FMRFamide also caused a
35 reduction of both outward currents in these centrifugal neurons. The fact that
36 FMRFamide reduced the magnitude of four of five characterized currents could
37 suggest that this neuropeptide may act as a strong inhibitory agent on these neurons.
38

39 **Introduction**

40 Among invertebrates, cephalopods are considered to have an extremely well-
41 developed eye and a centralized brain (Williamson and Chrachri, 2004), their retina
42 lacks the vertebrates equivalent of bipolar, amacrine, ganglion cells, etc. and therefore
43 there is very little visual processing within their retina which instead take place in the
44 optic lobe. Their retina contains only photoreceptors and supporting cells and it has
45 been demonstrated that there are some interconnection between the photoreceptors
46 (Yamamoto et al., 1965; Yamamoto and Takasu, 1984). There is also an extensive
47 efferent innervation of the retina coming from the inner granular layer of the cortex of
48 the optic lobe (Young, 1971 and 1974). These efferents are the axons of the
49 centrifugal neurons that have been demonstrated to be involved in the regulation of
50 the size of the receptive fields (Tasaki et al., 1982) and the control of the screening
51 pigment migration (Gleadall et al., 1993). This is still relatively simple compare to the
52 vertebrate retina.

53 Octopus seem to have a kind of camera eye with an iris and adjustable lens similar to
54 those of vertebrates, the retina consists of a single layer of photoreceptor cells, and the
55 optic lobe constitutes the center for visual analysis (Young, 1962). It has also been
56 suggested that the centrifugal neurons in the optic lobe project towards the
57 photoreceptors in the retina (Lund, 1979; Saidel, 1979). Although there is little data
58 about the neuromodulators contained in the centrifugal neurons, the presence of
59 several neurotransmitters and possible neuromodulators have already been observed in
60 the optic lobe (Cornwell et al., 1993; Di Cosmo and Di Cristo, 1998; Kito-Yamashita
61 et al., 1990; Sasayama et al., 1991; Suzuki and Yamamaoto, 2000 and 2002).

62 The neuropeptide FMRFamide (Phe-Met-Arg-Phe-NH₂) and similar molecules which
63 are collectively referred to as FMRFa-related peptides (FaRPs) first discovered in
64 molluscs (Price and Greenberg, 1977 and 1989) are conserved throughout the animal
65 phyla (Walker et al., 2009). They are abundant in both vertebrate and invertebrate
66 nervous systems (Espinoza et al., 2000; Dockray et al., 1983; O'Donohue et al., 1984;
67 Sorenson et al., 1984; Schneider and Taghert, 1988; Greenberg and Price, 1992;
68 Nelson et al., 1998). In these organisms, FMRFa-like neuropeptide act as
69 neurotransmitters and neuromodulators. In mammals, FMRFamide induces a variety
70 of physiological effects, including alterations in blood pressure, respiratory rate,

71 glucose-stimulated insulin release, and behavior (Mues et al., 1982; Sorenson et al.,
72 1984; Raffa et al., 1986; Thiemermann et al., 1991; Muthal et al., 1997; Nishimura et
73 al., 2000; Askwith et al., 2000). In cephalopods, it has been demonstrated that FMRFa
74 is involved in the control of egg laying in *Sepia officinalis* (Henry et al., 1999) as well
75 as the modulation of L-type calcium currents in heart muscle cells of squid (Chrachri
76 et al., 2000) and that of both the excitatory and inhibitory postsynaptic currents in
77 optic lobe neurones of cuttlefish (Chrachri and Williamson, 2003). In 1997, Loi and
78 Tublitz reported the isolation and characterization of a full-length FaRP cDNA from
79 the brain of cuttlefish, *Sepia officinalis*. The presence of FMRFa-like
80 immunoreactivity in the optic lobe of both octopus (Suzuki et al., 2002) and cuttlefish
81 (Chrachri and Williamson, 2003) has been reported indicating a putative
82 neurotransmitter or neuromodulator role for this neuropeptide. Furthermore, receptor
83 binding studies with squid optic lobes have identified G-protein associated FMRFa
84 binding sites (Chin et al., 1994). Although there have been reports of the ability of this
85 neuropeptide to modulate the activity of some cephalopod muscles (Loi and Tublitz,
86 2000; Chrachri et al., 2000) and to potentiate the activity at the squid giant synapse
87 (Cottrell et al., 1992). However, there is less understanding of its central function
88 (Chrachri and Williamson, 2003). In metazoans, different FMRFamide-Like Peptides
89 (FLP) types may exist in the same species, and the same FLP type may occur in
90 various species (Walker et al. 2009). Recently, a full-length cDNA sequence of an
91 FMRFamide gene isolated from the cuttlefish, *Sepia pharaonis* was cloned which
92 shares 93% and 92% similarity with two cuttlefish species, *Sepiella japonica* and
93 *Sepia officinalis* (Li et al., 2018; Zhu et al., 2020).

94 The mechanisms by which these FaRPs act are not yet fully understood. However, it
95 has been demonstrated that they either act directly on the membrane conductances of
96 excitable cells (Cottrell et al., 1984; Colombaioni et al., 1985; Belkin and Abrams,
97 1993) or through second messenger system (Brezina, 1988; Chiba et al., 1992; Raffa
98 and Stone, 1996; Chrachri et al., 2000). Furthermore, it has been also shown that
99 FMRFa can also activate directly one or more types of ligand-gated channels (Cottrell
100 et al., 1990; Chin et al., 1994; Green et al., 1994).

101 Although the morphology of the centrifugal neurons of the optic lobe of cephalopod
102 have been studied using both Golgi and cobalt chloride staining (Young, 1974; Saidel,

103 1979), there is no information on the types of ionic currents present in cephalopod
104 centrifugal neurons. This report provides the first comprehensive study of the voltage-
105 activated whole-cell membrane currents present in identified centrifugal neurons; we
106 have characterized five separate ionic currents in these neurons; two outward currents
107 and three inward currents and studied their modulation by the neuropeptide
108 FMRFamide.
109

110 **Material and methods**

111 ***Preparation of slices***

112 Slices were prepared from both male and female cuttlefish, *Sepia officinalis*. Animals
113 were anaesthetized with 2% ethanol and sacrificed by decapitation. The optic lobe was
114 rapidly removed and placed in ice-cold Ca^{2+} -free artificial sea water (ASW).
115 Transverse slices of around 300 μm were cut with a vibratome (Campden Instruments,
116 Loughborough, UK). Slices were kept in a storage chamber in the fridge for up to 1 h
117 before recording.

118 ***Electrophysiological recordings***

119 Individual slices were transferred to the recording chamber, they were fully
120 submerged and superfused with oxygenated ASW at a rate of 2-3 ml/min. Centrifugal
121 neurons were visually identified using an Olympus BX50WI upright microscope with
122 a x40 water immersion objective lens and equipped with infrared illumination and
123 video enhanced visualization system consisting of a CCD camera (C7500) and its
124 controller (C2741-90, Hamamatsu Photonics Ltd., Hertfordshire, UK).

125 Identified centrifugal neurons were studied at room temperature (18-20 °C) with the
126 whole-cell patch recording techniques (Hamill et al., 1981). Recordings were made
127 using an Axopatch amplifier (200A, Molecular devices, San Jose, CA 95134, USA)
128 controlled by PClamp8 software (Molecular devices) for data acquisition, analysis and
129 storage. Ionic currents were sampled at a rate of 10 kHz and were low-pass filtered at
130 2 kHz. The pipette series resistance was electronically compensated, as far as possible,
131 to give voltage errors of only few mV at peak current levels. The capacitance current
132 response to a -10 mV voltage step, from a holding potential of -60mV, was recorded
133 for each neuron and the access resistance calculated. Liquid junction potential was
134 calculated using the liquid junction calculator provided by the PClamp software. Patch
135 electrodes with tip resistance of 4.0–6.0 M Ω were pulled using a horizontal puller
136 (Sutter Model P-97, Novato, CA, USA) from soda glass capillaries (Intracel, 1.5 mm
137 o.d., 0.86 mm i.d.). These electrodes were filled with either Aspartate or CsCl_2 based
138 internal solution.

139 ***Solution and drugs***

140 The artificial sea water contained (in mM): 430 NaCl; 10 KCl; 10 CaCl_2 ; 30 MgCl_2 ;
141 25 MgSO_4 ; 0.5 KH_2PO_4 ; 2.5 NaHCO_3 ; 10 Glucose; 10 HEPES buffer at pH 7.8,

142 osmolarity = 997 mO. Other solutions were made by equimolar substitution of this
143 basic formula. For example, calcium chloride was replaced with barium chloride to
144 enhance the inward L-type calcium current. For the calcium free ASW magnesium
145 was substituted for calcium. Patch pipettes were filled with a solution containing
146 (mM): 500 Aspartate or CsCl₂; 10 NaCl; 4 MgCl₂; 3 EGTA; 20 HEPES, 2 Na₂ATP,
147 0.2 Na₃GTP, 0.2 Lucifer Yellow CH (lithium salt), pH and osmolarity were adjusted
148 to 7.4 and 870 Osm mol kg⁻¹ H₂O with KOH and sucrose, respectively.

149 Pharmacological agents used to block the characterized ionic currents were purchased
150 from Sigma-Aldrich (Gillingham Dorset, England). These included tetrodotoxin
151 (TTX), tetraethylammonium chloride (TEA⁺), 4-aminopyridine (4AP), cesium
152 chloride (CsCl₂), cobalt chloride (CoCl₂), barium chloride (BaCl₂), nifedipine was
153 dissolved in absolute ethanol to make 5 mM stock solutions and stored at 5 °C in the
154 dark. Experiments with nifedipine were carried out in dim light to prevent photo-
155 oxidation. FMRFa was bath applied approximately 10 min after whole cell membrane
156 seal and break-in.

157 ***Statistics***

158 The software package InStat was used for statistical analysis. All data are given as
159 mean ± SE. Where statistical comparisons are made before and after bath application
160 of FMRFa, then the two-tailed paired student's *t*-test was employed. If not stated
161 otherwise, data were denoted as statistically significant when $P < 0.05$.

162

163 **Results**

164 The morphology of a typical centrifugal neuron located in the inner granule cell layer
165 of the optic lobe as revealed by Lucifer yellow staining through the recording
166 microelectrode is shown in Fig. 1A. These efferent cells have a single axon that
167 crosses the major neuropil area in the plexiform zone and then exits into one of the
168 optic nerve bundles. These centrifugal neurons always give off a number of laterally
169 running branches within the plexiform zone (arrowheads, Fig. 1A) without branching
170 outside this zone. Their long axon can be seen leaving the slice (Fig. 1A). These cells
171 can be provisionally identified visually in living slices of the optic lobe based on their
172 size and position and hence can be readily selected for electrophysiological study and
173 their identity is further verified from their responses to optic nerve bundle stimulation
174 which always evoked an antidromic action current and also by dye filling them
175 through the patch pipette.

176 In cell-attached mode which provides a way not only to record the activity, but also to
177 stimulate neurons in brain slice preparations. Furthermore, cell-attached recording of
178 action potential currents is an easy type of recording to do because no breaking of the
179 patch is involved, and the seal can be loose ($< 1 \text{ G}\Omega$; Kondo and Marty, 1998). Using
180 this mode of recording action potential current can be evoked by stimulating the
181 appropriate optic nerve (Fig1. B).

182 Whole-cell patch clamp recordings were obtained from identified centrifugal neurons,
183 depolarizing pulses of 80 ms duration, from a holding potential of -60 mV, were used
184 to set the membrane potential at voltages ranging from -60 mV to +60 mV with a 10
185 mV increments which elicited two main categories of currents; a large outward
186 current (*open circle*) and an inward current which had an initial large transient
187 component (*filled circle*) followed by a smaller inward current (*filled triangle*. Fig1.
188 C). The current-voltage (I-V) curves showing the outward current (*open circles*) and
189 the fast inward current (*filled circles*, Fig. 1D).

190 ***Whole-cell outward currents***

191 The large outward current observed in these centrifugal neurons at depolarized
192 potentials was studied using aspartate internal solution in the pipette as well as 1 μM
193 TTX and 2 mM CoCl_2 in the external solution to block both the sodium and calcium
194 currents respectively. In this study, we found that in 84% of the centrifugal neurons

195 (21 out of 25) displayed two components of the outward current; a transient fast-
196 inactivating component and a sustained component (Fig. 2A). In the remaining 16%
197 (4 neurons), only the sustained component was observed. These two components of
198 the outward current could be separated using either their voltage or pharmacological
199 sensitivities (Connor and Stevens, 1971 a, b). If the cell was held at a holding
200 potential of -40 mV instead of -60 mV, the initial transient component (Fig. 2A)
201 disappeared during the voltage step protocol (Fig. 2B). Subtracting the outward
202 currents recorded at -40 mV from those recorded at -60 mV revealed the shape of the
203 transient or A-current (Fig. 2C). The current-voltage relationships at these two holding
204 potentials (-40 and -60 mV) as well as the isolated transient or A-current (I_A) are
205 illustrated in Fig. 2D. The addition of 4AP (4 mM) to the bathing solution also
206 abolished the large transient component of the outward current, leaving only the
207 sustained outward current (bold trace, Fig. 2E). The current-voltage relationships for
208 these currents are shown in Fig. 2F. The remaining outward current after either
209 voltage (Fig. 2B) or pharmacological (Fig. 2E) separation has a sustained time course
210 and is similar to the delayed rectifier (I_K) of other nerve cells. This is confirmed by its
211 reduction (75%) in the presence of TEA (20 mM, Fig. 2E). These results are
212 consistent with the presence of two separate outward currents, which from their
213 kinetics, current-voltage curves, and pharmacological sensitivities, can be
214 characterized as those already reported outward currents in many preparations,
215 namely, the delayed rectifier (I_K) and the transient A-current (I_A).

216 ***Whole-cell inward currents***

217 Inward currents were studied using cesium chloride for the pipette filling solution to
218 block most of the outward potassium currents we have described above. Under these
219 conditions, two inward currents were observed in centrifugal neurons of the optic lobe
220 slice (Fig. 3). The first one had a transient time course (Fig. 3A, star) and the second
221 had a more sustained time course (Fig. 3A, S). The transient inward current can be
222 blocked by the addition of TTX (1 μ M) to the bathing solution, leaving only a
223 sustained inward current (Fig. 3B). TTX is a known blocker of sodium currents in
224 many different animal cell types (Hill, 1992). Subtracting current traces after the
225 application of TTX (Fig. 3B) from those recorded before revealed the TTX-sensitive
226 current (Fig. 3C). The current-voltage relationships (not shown) of this transient

227 inward current appeared at potentials more positive than -50 mV, peaked at around -
228 20 mV, and then starts decreasing. Three lines of evidence indicate that this fast
229 transient inward current is sodium current (I_{Na}). Firstly, it was blocked by TTX (Fig.
230 3B); secondly, it was also blocked in the presence of a sodium-free saline such
231 replacing sodium with lithium or choline chloride (data not shown); and thirdly, this
232 inward current could be progressively inactivated by setting the holding potentials at
233 values more positive than -40 mV. Taken together these data suggest that this current
234 is probably the sodium current responsible for the rising phase of the action potential
235 generation.

236 The second inward current had a sustained time course and was not affected either by
237 TTX (Fig. 3B) or by a sodium-free saline (not shown) and could be increased by the
238 substituting barium for calcium in the ASW (Fig. 4A). This current could be totally
239 blocked by the addition of cobalt chloride (2 to 4 mM) to the external solution (Fig.
240 4B), or cadmium chloride (data not shown) suggesting that it could be carried by
241 calcium ions. Furthermore, this inward current was more importantly blocked by the
242 dihydropyridine antagonist, nifedipine, at a concentration of 5 μ M (Fig. 4C) which
243 strongly suggest that this current is probably an L-type calcium current ($I_{Ca,L}$). The
244 current-voltage relationships of this inward calcium current demonstrated that it was
245 rapidly activated by voltage steps more positive than -40 mV and was maintained
246 throughout the voltage step with no sign of inactivation. This sustained inward current
247 achieved a maximum for test steps around 0 or +10 mV and then decreased. In some
248 of our experiments, a third inward current which was also carried by calcium, but can
249 be seen only with test pulses from negative holding potential ($V_h = -80$ mV) had a
250 transient time course compared to the L-type calcium current (Fig. 4D, trace a). The
251 current-voltage relationships plot shown in Fig 4E (filled triangles) show that this
252 current starts to activate at around -50 mV, its amplitude increased progressively with
253 higher depolarizations, reaching a plateau around -30 mV and then began to decrease.
254 This current is usually referred to as T-type calcium current ($I_{Ca,T}$) because of its
255 transient time course. This current is blocked when the holding potential is set at -60
256 mV or above (Fig. 4D, trace b). This current is similar to the one that have been
257 reported in heart muscles of squid (Ödblom et al. 2000). In these centrifugal neurons,
258 the L-type calcium was encountered invariably. By contrast, the T-type calcium

259 currents were rare and we have only seen them in 5 centrifugal neurons. This transient
260 inward current had similar pharmacological characteristics to that of reported in heart
261 muscle cells of squid (Ödblom et al., 2000; Chrachri et al., 2000), in that it was only
262 partially blocked by 2-5 μM nifedipine. This dihydropyridine antagonist has been
263 shown to block preferentially the L-type calcium current in many preparations (Fox et
264 al., 1987; Wang et al., 1996; Chrachri and Williamson, 1997). However, as for the
265 isolated heart muscle cells, nifedipine also blocks the transient calcium current by
266 about 48.4% ($n = 3$).

267 ***Effect of FMRFa on the outward current***

268 To investigate the effect of the neuropeptide FMRFa on the outward potassium
269 currents in the centrifugal neurons, we bath applied FMRFa (1 μM) to voltage
270 clamped centrifugal neurons and found that this neuropeptide induced a significant
271 reduction of the overall potassium current in 11 out of 15 centrifugal neurons. At a
272 holding potential of -60 mV, the reduction of the potassium currents was significant (p
273 < 0.0001) and was about $39.83 \pm 7.92\%$ ($n = 11$). When the holding potential was set
274 to -40 mV and therefore to study the effect of FMRFa on the delayed rectifier (I_k) on
275 its own, the reduction of I_k by FMRFa was also reduced significantly ($p = 0.0028$) by
276 about $31.27 \pm 10.45\%$ ($n = 5$). A typical experiment demonstrating the FMRFa-
277 induced reduction of the peak current of both the fast-inactivating and sustained
278 potassium currents is illustrated in Fig. 5. The effect of FMRFa on these two
279 components of the potassium currents was reversible (Fig. 5C). Subtracting the
280 current traces in the presence of FMRFa (Fig. 5B) from the control current traces (Fig.
281 5A) revealed the FMRFa-sensitive potassium currents (Fig. 5D). In the remaining 4
282 centrifugal neurons, FMRFa did not appear to have any apparent effect on both
283 components of the outward potassium current (data not shown).

284 ***FMRFa-mediated attenuation of the inward sodium current (I_{Na})***

285 Bath application of FMRFa (1 μM) seems to induce a reduction in the magnitude of
286 this inward sodium current. Fig. 6A illustrates a typical example, 5 minutes after bath
287 application of FMRFa the amplitude of the sodium current was reduced by about
288 28.8% (Fig. 6A, grey line). 8 minutes after the addition of FMRFa, the amplitude of
289 I_{Na} was reduced even further, this time by about 44.44% (Fig. 6A, thick line). The
290 effect of FMRFa on the I_{Na} is also illustrated in Fig. 6B, where the current-voltage

291 relationship demonstrates that FMRFa reduces I_{Na} over most of the voltage ranges.
292 Pooled data from 3 experiments demonstrated that FMRFa induced a significant ($p =$
293 0.01) decrease of the sodium current by about $41.74 \pm 5.94\%$.

294 ***Effect of FMRFa on L-type and T-type calcium currents***

295 Fig. 6, not only demonstrates that FMRFa reduced the peak amplitude of the I_{Na} (star),
296 but also decreased that of the sustained L-type calcium current (triangle). Unlike in the
297 case of potassium currents, bath application of FMRFa ($1 \mu\text{M}$) always resulted in
298 reducing the calcium current. The magnitude of the peak $I_{Ca,L}$ was reduced
299 significantly ($p = 0.0002$) by about $64.92 \pm 5\%$ ($n = 8$). An example is illustrated in
300 Fig. 7A (right panel), where the inhibition of $I_{Ca,L}$ was about 52%. The current-voltage
301 curves show that FMRFa reduction of the amplitude of $I_{Ca,L}$ is over most of the
302 voltage ranges. However, the reduction induced by FMRFa decreased for steps to
303 depolarized voltages more positive than +10 mV (Fig. 7B). This figure also
304 demonstrates that FMRFa ($1 \mu\text{M}$) didn't have any noticeable effect on the T-type
305 calcium current (Fig. 7A, left panel). The current/voltage plot provides further
306 evidence that FMRFa selectively affects the amplitude of $I_{Ca,L}$, but not the $I_{Ca,T}$ (grey
307 circles, Fig. 7B). Figure 8 illustrates the time course of the onset of the inhibition of
308 $I_{Ca,L}$ by FMRFamide and the subsequent recovery by washing, and demonstrates that
309 the inhibition was relatively rapid and fully reversible.

310

311 **Discussion**

312 This study has characterized the electrical properties in identified centrifugal neurons
313 in the optic lobe slice preparation of the cuttlefish, *Sepia officinalis*, using whole-cell
314 patch clamp we documented the presence of five voltage-sensitive ionic currents and
315 studied their modulation by the neuropeptide FMRFa. These voltage-activated
316 currents comprised; tree inward currents; one carried by sodium (I_{Na}) and the two
317 others by calcium (I_{CaL} and I_{CaT}), and two outward currents that were selective for
318 potassium (I_A , I_K). The effect of the neuropeptide, FMRFa, on these currents is also
319 discussed.

320 *Na⁺ current*

321 The rapid inward current is activated immediately after the onset of the command
322 pulse, reaches a peak in few milliseconds, and inactivated within 10 ms. As in many
323 other excitable tissues (Lo and Shrager, 1981; Neher, 1971; Lasater, 1986), this fast
324 inward current is carried by sodium, in that it is blocked when the optic lobe slice is
325 perfused with a sodium-free ASW, it is also totally blocked by TTX (1 μ M) and is
326 inactivated when the cells is held at values more positive than -40 mV. This I_{Na} was
327 present in all of the centrifugal neurons we have recorded from (without exception).
328 The presence of such sodium current in these centrifugal neurons was not surprising
329 because these neurons send their axons a long distance towards the retina (Saidel,
330 1979) and therefore it is possible that these centrifugal neurons will need action
331 potentials to carry their information towards the photoreceptors located in the retina.
332 Whole-cell patch clamp recordings from other cell types within the optic lobe (i.e.
333 medulla and amacrine) demonstrated that these neurons do not extend their axons
334 towards the retina, and that only a few of them displayed sodium currents it is present
335 in only about a third of them (Chrachri and Williamson, unpublished data).

336 *Ca²⁺ currents*

337 A vast amount of investigations have been carried out on the voltage-dependent
338 calcium currents in a variety of neuron and muscle cells (Liu and Lasater, 1994;
339 Ödblom et al., 2000). In the present investigation we have identified two more inward
340 currents, one of which have a sustained time course and the other have a transient time
341 course. Both of them were carried by calcium ions (Fig. 4). On the basis of its
342 kinetics, ion specificity and pharmacological sensitivity, the sustained inward current

343 resembles to the high voltage-activated calcium (HVA), or L-type calcium current
344 reported in a variety of other cell types (Carbone and Lux 1984,; Fox et al., 1987). The
345 other voltage-dependent calcium current is similar to the transient, low-threshold
346 (LVA) or T-type (Nowycky et al., 1985) which only appeared when neurons were held
347 at potentials more negative than -60 mV. This current had similar kinetics and
348 pharmacological characteristics to that reported in squid isolated heart muscle cells
349 (Ödholm et al., 2000; Chrachri et al., 2000), in that it showed higher selectivity to
350 blockade by nickel chloride than the L-type calcium current (data not shown) which is
351 similar to reports in other preparations (Mitra and Morad, 1986; Hagiwara et al., 1988;
352 Wu and Lipsius, 1990). It was also partially blocked by nifedipine which has been
353 shown to have a more specific effect on the L-type calcium current (Scott et al., 1991),
354 but similar results have been reported in atrial cells (Bean, 1985), retinal ganglion
355 cells (Liu and Lasater, 1994) and olfactory bulb neurons (Wang et al., 1996).

356 *K⁺ currents*

357 Under voltage-clamp conditions, when centrifugal neurons were depolarized to
358 voltages more positive than -30 mV from a holding potential of -60 mV, two outward
359 potassium currents were detected, the delayed rectifier or I_K and the A-current or I_A .
360 These two time- and voltage-dependent K^+ currents were distinguishable both by their
361 pharmacological sensitivity to 4AP, and by their voltage-dependent inactivation
362 (Connor and Stevens, 1971 a, b; Thompson, 1977). Similar results have been reported
363 in other cephalopod cells (Llano and Bookmanm, 1986; Lucero et al., 1992; Chrachri
364 and Williamson, 1997). TEA at a concentration of 20 mmol l⁻¹ blocked most of the
365 delayed rectifier K^+ currents in centrifugal neurons. These concentrations of TEA are
366 relatively very low compared to those needed to block the similar I_K in sensory hair
367 cells of the squid statocysts (Chrachri and Williamson, 1997), the squid giant axons
368 (Tasaki and Hagiwara, 1957) and isolated heart muscle cells (Ödholm et al., 2000)
369 where very high concentrations of TEA were needed. The delayed rectifier activates at
370 potentials more positive than does the A-type current and show no appreciable
371 inactivation during a depolarizing voltage step also contribute to action potential
372 repolarization (Saito and Wu, 1991). The effects of blockade of delayed rectifier in
373 centrifugal neurons by TEA are consistent with the pharmacology of other delayed-
374 rectifier subtypes of K^+ channels (see Hille, 1992).

375 *FMRFa-mediated effect on the centrifugal neurons of the optic lobe*

376 We have demonstrated that the neuropeptide, FMRFa, significantly reduced the
377 inward Na^+ current in the centrifugal neurons of the optic lobe, the effect was voltage
378 dependent, it lasts as long as the peptide is present and finally the reduction of Na^+
379 current by FMRFa is partially reversible. Furthermore, This FMRFa-induced
380 inhibition was also seen as a reduction of the antidromic action current following
381 stimulation of the appropriate optic nerve bundle (not shown). Modulation of Na^+
382 current is likely to be important in the regulation of the centrifugal neuron's
383 excitability. The reduction of the I_{Na} by FMRFa will increase the threshold of the
384 action potential and so contribute to the inhibitory effects of FMRFa on the
385 excitability of the cell, possibly resulting in suppressing on-going firing activity as
386 well as preventing the generation of new discharges. Inhibition of this current by
387 FMRFa has been shown in other molluscan preparations, the peptidergic caudo-dorsal
388 cells of the mollusc *Lymnaea stagnalis* (Brussaard et al., 1991).

389 Another action of FMRFa is to attenuate the voltage-dependent sustained calcium
390 current. Attenuation of this type of calcium current by FMRFa has also been described
391 in a number of other types of cells (Kramer et al., 1988; Man-Song-Hing et al., 1989;
392 Yakel, 1991; Chrachri et al., 2000). However, this neuropeptide didn't have any effect
393 on the T-type calcium current. Similar selectivity for the FMRFamide-induced
394 reduction of the calcium current has been reported in neurons of *Aplysia californica*
395 (Brezina et al., 1987), in isolated heart muscle cells of squid (Chrachri et al., 2000). It
396 is probably not surprising that FMRFa affected $I_{\text{Ca,L}}$ but not $I_{\text{Ca,T}}$ in centrifugal
397 neurons. It has been reported that this neuropeptide reduced the amplitude of
398 spontaneous excitatory postsynaptic currents (sEPSCs) in centrifugal neurons.
399 However, when these sEPSCs occurred in bursting mode, FMRFa did change the
400 amplitude of sEPSCs without any significant modulation of the frequency their
401 rhythmic activity (Chrachri unpublished data). This transient current has been
402 proposed to control rhythmic membrane oscillations central neurons (Llinas and
403 Yarom, 1981) and therefore the lack of effect of FMRFa on $I_{\text{Ca,T}}$ might have been
404 expected.

405 We have also presented evidence that application of FMRFa evoked a partial blockade
406 of both characterized outward; the I_A as well as the I_{kv} currents in these
407 morphologically identifiable centrifugal neurons of the optic lobe.

408 *Physiological relevance of the action of FMRFa*

409 The reduction of the amplitude of the L-type calcium current in the centrifugal
410 neurons would be a relevant physiological action for FMRFa. Ca^{2+} channels in
411 neurons are frequent targets of neurotransmitter modulation, with suppression or
412 enhancement of Ca^{2+} channel activity being a common outcome, albeit *via* different
413 mechanisms (Gerschenfeld et al., 1989; Yakel, 1991). The fact that this neuropeptide
414 affect the ionic currents (this study) and the postsynaptic currents of these efferent
415 neurons (Chrachri and Williamson, 2003) would undoubtedly suggest a role for the
416 retinal cells which are under the control of these centrifugal neurons (Saidel, 1979).
417 There is a wide distribution of FMRFa like immunoreactivity in the optic lobe of
418 cephalopods (Suzuki et al., 2002; Chrachri and Williamson, 2003). Thus the FMRFa-
419 induced effects on the centrifugal neurons we have reported in this paper may
420 probably mirror the endogenous modulation of the centrifugal neuron by
421 FMRFamidergic nerve fibres. Using behavioral studies it has been demonstrated that
422 the optic lobe of *sepia officinalis* may provides a system for coding, sorting and
423 decoding the visual input to produce a relevant behaviour (Chichery and Chanelet,
424 1976). The fact that the application of FMRFa induced not only a modulation of ionic
425 currents (this report), but also appears to act presynaptically to modulate both
426 spontaneous excitatory and inhibitory currents in the same preparation (Chrachri and
427 Williamson, 2003) could suggest that this neuropeptide may play a crucial role in
428 visual processing. Similar roles for FMRFa in visual processing have been described
429 in the locust optic lobe (Rémy et al., 1988) and in fish (Wang et al., 2000).

430

431

432

433 **List of symbols and abbreviations**

434 o.gr.: outer granule cell layer; i.gr.: inner granule cell layer; pl: plexiform zone; 4AP:
435 4-aminopyridine; TEA: tetra-ethyl ammonium; TTX: tetrodotoxin

436 **Competing interests**

437 I declare that there are no competing or financial interests.

438 **Funding**

439 This work was supported by the Wellcome Trust.

440

441 **References**

- 442 **Askwith, C. C., Cheng, C., Ikuma, M., Benson, C. and Welsh, M. J.** (2000).
443 Neuropeptide FF and FMRFamide potentiate acid-evoked currents from sensory
444 neurons and proton-gated DEG/ENaC channels. *Neuron* **26**, 133-141. doi:
445 [10.1016/s0896-6273\(00\)81144-7](https://doi.org/10.1016/s0896-6273(00)81144-7)
- 446 **Bean, B. P.** (1985). 2 kinds of calcium channels in canine atrial cells- differences in
447 kinetics, selectivity and pharmacology. *J. Gen. Physiol.* **86(1)**, 1-30. doi:
448 [10.1085/jgp.86.1.1](https://doi.org/10.1085/jgp.86.1.1)
- 449 **Belkin, K. J. and Abrams, T. W.** (1993). FMRFamide produces biphasic modulation
450 of the LFS motor-neurons in the neural circuit of the siphon withdrawal reflex of
451 *Aplysia* by activating Na⁺ and K⁺ currents. *J. Neurosci.* **13**, 5139-5152
452 doi.org/10.1523/JNEUROSCI.13-12-05139.1993
- 453 **Brezina, V., Eckert, R. and Erxleben, C.** (1987). Suppression of calcium current by
454 endogenous neuropeptide in neurones of *Aplysia californica*. *J. Physiol. (Lond)* **388**,
455 565-595. doi: [10.1113/jphysiol.1987.sp016632](https://doi.org/10.1113/jphysiol.1987.sp016632)
- 456 **Brezina, V.** (1988). Guanosine 5'-triphosphate analog activates potassium current
457 modulated by neurotransmitters in *Aplysia* neurons. *J. Physiol. (Lond)* **407**, 15-40.
458 doi.org/10.1113/jphysiol.1988.sp017401
- 459 **Brussaard, A.B., Lodder, J. C., Termaat, A., Devlieger, T. A. and, Kits, K. S.**
460 (1991). Inhibitory modulation by FMRFamide of the voltage-gated sodium current in
461 identified neurons in *Lymnaea stagnalis*. *J. Physiol. (Lond)* **441**, 385-404. doi:
462 [10.1113/jphysiol.1991.sp018757](https://doi.org/10.1113/jphysiol.1991.sp018757)
- 463 **Carbone, E. and Lux, H. D.** (1984). A low voltage-activated fully inactivating Ca
464 channel in vertebrate sensory neurones. *Nature (Lond)* **310**, 501-502. doi:
465 [10.1038/310501a0](https://doi.org/10.1038/310501a0)
- 466 **Chiba, O., Sasaki, K., Higuchi, H. and Takashima, K.** (1992). G-protein mediating
467 the slow depolarization induced by FMRFamide in the ganglion cells of *Aplysia*.
468 *Neurosci. Res.* **15**, 255-264. doi: [10.1016/0168-0102\(92\)90046-f](https://doi.org/10.1016/0168-0102(92)90046-f)
- 469 **Chin, G. J., Payza, K., Price, D. A., Greenberg, M. J. and Doble, K. E.** (1994)
470 Characterization and solubilization of the FMRFamide receptor of squid. *Biol. Bull.*
471 **187**, 185-199. doi: [10.2307/1542241](https://doi.org/10.2307/1542241)

- 472 **Chichery, R. and Chanelet, J.** (1976). Motor and behavioral responses obtained by
473 stimulation with chronic electrodes of the optic lobe of *Sepia officinalis*. *Brain Res.*
474 **105**, 525-32. [doi.org/10.1016/0006-8993\(76\)90598-9](https://doi.org/10.1016/0006-8993(76)90598-9)
- 475 **Chrachri, A. and Williamson, R.** (1997). Voltage-dependent conductances in
476 cephalopod primary sensory hair cells. *J. Neurophysiol.* **78**, 3125-3132.
477 doi.org/10.1152/jn.1997.78.6.3125
- 478 **Chrachri, A., Ödöblom, M. and Williamson, R.** (2000). G protein-mediated
479 FMRFamideergic modulation of calcium influx in dissociated heart muscle cells from
480 squid, *Loligo forbesii*. *J. Physiol. (Lond)* **525** (2), 471-482. [doi: 10.1111/j.1469-](https://doi.org/10.1111/j.1469-7793.2000.00471.x)
481 [7793.2000.00471.x](https://doi.org/10.1111/j.1469-7793.2000.00471.x)
- 482 **Chrachri, A. and Williamson, R.** (2003). Modulation of spontaneous and evoked
483 EPSCs and IPSCs in optic lobe neurons of cuttlefish, *Sepia officinalis* by the
484 neuropeptide FMRF-amide. *Eur. J. Neurosci.* **17** (3), 526-536.
485 doi.org/10.1046/j.1460-9568.2003.02478.x
- 486 **Colombaioni, L., Paupardin-Tritsch, D., Vidal, P. P. and Gerschenfeld, H. M.**
487 (1985). The neuropeptide FMRF-amide decreases both the Ca²⁺ conductance and a
488 cyclic 3',5'-adenosine monophosphate-dependent K⁺ conductance in identified
489 molluscan neurones. *J. Neurosci.* **5**, 2533-2538. [doi.org/10.1523/JNEUROSCI.05-09-](https://doi.org/10.1523/JNEUROSCI.05-09-02533)
490 [02533](https://doi.org/10.1523/JNEUROSCI.05-09-02533)
- 491 **Connor, J. A. and Stevens, C. F.** (1971a). Inward and delayed outward membrane
492 currents in isolated neural somata under voltage-clamp. *J. Physiol. (Lond)* **213**:1-19.
493 doi.org/10.1113/jphysiol
- 494 **Connor, J. A. and Stevens, C. F.** (1971b) Voltage-clamp studies of a transient
495 outward current in a gastropod neural somata. *J. Physiol. (Lond)* **213**, 21-30. [doi:](https://doi.org/10.1113/jphysiol.1971.sp009365)
496 [10.1113/jphysiol.1971.sp009365](https://doi.org/10.1113/jphysiol.1971.sp009365)
- 497 **Cornwell, C.J., Messenger, J.B. and Williamson, R.** (1993). Distribution of GABA-
498 like immunoreactivity in the octopus brain, *Brain Res.* **621**, 353-357.
499 [doi.org/10.1016/0006-8993\(93\)90127-9](https://doi.org/10.1016/0006-8993(93)90127-9)
- 500 **Cottrell, G. A., Davies, N. W. and Green, K. A.** (1984). Multiple actions of a
501 molluscan cardioexcitatory neuropeptide and related peptides on identified *Helix*
502 neurones. *J. Physiol. (Lond)* **356**, 315-333. doi.org/10.1113/jphysiol

- 503 **Cottrell, G. A., Green, K. A. and Davies, N. W.** (1990). The neuropeptide
504 FMRFamide can activate a ligand-gated ion channel in *Helix* neurones. *Pflügers Arch.*
505 **416**, 612-614. doi: [10.1007/BF00382698](https://doi.org/10.1007/BF00382698)
- 506 **Cottrell, G. A., Lin, J. W., Llinas, R., Price, D. A., Sugimori, M. and Stanley, E.**
507 **F.** (1992). FMRF-amide-related peptides potentiate transmission at the squid giant
508 synapse. *Exp. Physiol.* **77**, 881-889. doi.org/[10.1113/expphysiol](https://doi.org/10.1113/expphysiol)
- 509 **Di Cosmo, A. and Di Cristo, C.** (1998). Neuropeptidergic control of the optic gland
510 of *Octopus vulgaris*: FMRF-amide and GnRH immunoreactivity, *J. Comp. Neurol.*
511 **398**, 1-12. doi: [10.1002/\(sici\)1096-9861\(19980817\)398:1<1::aid-cne1>3.0.co;2-5](https://doi.org/10.1002/(sici)1096-9861(19980817)398:1<1::aid-cne1>3.0.co;2-5)
- 512 **Dockray, G. J., Reeve, J. R., Shively, J., Gayton, R. J. and Barnard, C. S. A.**
513 (1983) Novel active peptide from chicken brain identified by antibodies to
514 FMRFamide. *Nature* **305**: 328-330. doi: [10.1038/305328a0](https://doi.org/10.1038/305328a0)
- 515 **Espinoza, E., Carrigan, M., Thomas, S.G., Shaw, G. and Edison, A.S.** (2000). A
516 statistical view of FMRFamide neuropeptide diversity. *Mol. Neurobiol.* **21**, 35–56.
517 doi: [10.1385/MN:21:1-2:035](https://doi.org/10.1385/MN:21:1-2:035)
- 518 **Fox, A. P., Nowycky, M. C. and Tsien, R. W.** (1987). Kinetic and pharmacological
519 properties distinguishing three types of calcium currents in chick sensory neurones. *J.*
520 *Physiol. (Lond)* **394**, 149-172. doi: [10.1113/jphysiol.1987.sp016864](https://doi.org/10.1113/jphysiol.1987.sp016864)
- 521 **Gerschenfeld, H. M., Paupardin-Tritsch, D., Hammond, C. and Harris-Warrick,**
522 **R.** (1989) Intracellular mechanism of neurotransmitter-induced modulations of
523 voltage-dependent Ca²⁺ current in snail neurons. *Cell. Biol. Int. Rep.* **13 (12)**, 1141-
524 1154. doi.org/[10.1016/0309-1651\(89\)90028-3](https://doi.org/10.1016/0309-1651(89)90028-3)
- 525 **Gleadall, I. G., Ohtsu, K., Gleadall, E. and Tsukahara, Y.** (1993). Screening-
526 pigment migration in the *Octopus* retina includes control by dopaminergic efferents. *J.*
527 *Exp. Biol.* **185**, 1-16. . <http://jeb.biologists.org/content/185/1/1>
- 528 **Green, K. A., Falconer, S. W. and Cottrell, G. A.** (1994). The neuropeptide Phe-
529 Met-Arg-Phe-NH₂ (FMRFamide) directly gates two ion channels in an identified
530 *Helix* neurone. *Pflügers Arch.* **428**, 232-240. doi: [10.1007/BF00724502](https://doi.org/10.1007/BF00724502)
- 531 **Greenberg, M. J. and Price, D. A.** (1992). Relationships among the FMRFamide-
532 like peptides. *Prog. Brain Res.* **92**, 25-37. doi: [10.1016/s0079-6123\(08\)61162-0](https://doi.org/10.1016/s0079-6123(08)61162-0)

- 533 **Hagiwara, N., Irishawa, H. and Kameyama, M.** (1988). Contribution to two types
534 of calcium currents to pacemaker potentials of rabbit sinoatrial node cell. *J. Physiol.*
535 (*Lond*) **395**, 233-253. <https://doi.org/10.1113/jphysiol>
- 536 **Hamill, O. P., Marty, A., Neher, E., Sackmann, B. and Sigworth, F. J.** (1981).
537 Improved patch-clamp and cell-free membrane patches. *Pflügers Arch* **391**:91-100.
538 [doi: 10.1007/BF00656997](https://doi.org/10.1007/BF00656997)
- 539 Henry J, Zatylny C Boucaud-Camou E (1999) Peptidergic control of egg-laying in the
540 cephalopod *Sepia officinalis*: involvement of FMRFamide and FMRFamide-related
541 peptides. *Peptides* **20(9)**, 106-1070. [doi: 10.1016/s0196-9781\(99\)00102-3](https://doi.org/10.1016/s0196-9781(99)00102-3)
- 542 **Hille, B.** (1992). Ionic channels of excitable membranes. Sinauer, Sunderland, MA.,
543 **Kito-Yamashita, T., Haga, C., Hirai, K., Uemura, T., Kondo, H. and Kosaka, K.**
544 (1990). Localization of serotonin immunoreactivity in cephalopod visual system,
545 *Brain Res.* **521**, 81–88. [doi: 10.1016/0006-8993\(90\)91527-n](https://doi.org/10.1016/0006-8993(90)91527-n)
- 546 **Kondo, S. and Marty, A.** (1998). Synaptic currents at individual connections among
547 stellate cells in rat cerebellar slices. *J. Physiol.* **509**, 221-232
548 <https://doi.org/10.1111/j.1469-7793.1998.233bo.x>
- 549 **Kramer, R., Levitan E., Carrow G. and Levitan I.** (1988). Modulation of a
550 subthreshold calcium current by the neuropeptide FMRFamide in Aplysia neuron. *J.*
551 *Neurophysiol.* **60**, 1728-1738. doi.org/10.1152/jn.1988.60.5.1728
- 552 **Lasater, E. M.** (1986). Ionic currents of cultured horizontal cells isolated from white
553 perch retina. *J. Neurophysiol.* **55**, 499-513. doi.org/10.1152/jn.1986.55.3.499
- 554 **Li, Y., Cao, Z., Li, H., Liu, H., Lü, Z. and Chi, C.** (2018). Identification,
555 Characterization, and Expression Analysis of a FMRFamide-Like Peptide Gene in the
556 Common Chinese Cuttlefish (*Sepiella japonica*). *Molecules* **23**, 742;
557 [doi:10.3390/molecules23040742](https://doi.org/10.3390/molecules23040742)
- 558 **Liu, Y. and Lasater, E. M.** (1994). Calcium currents in turtle retinal ganglion cells. I.
559 The properties of T- and L-type currents. *J. Neurophysiol.* **71**, 733-742.
560 doi.org/10.1152/jn.1994.71.2.733
- 561 **Llano, I. and Bookman, R. J.** (1986). Ionic conductances of squid giant fiber lobe
562 neurons. *J. Gen. Physiol.* **88**, 543-569. [doi: 10.1085/jgp.88.4.543](https://doi.org/10.1085/jgp.88.4.543)

- 563 **Llinas, R. and Yarom, Y.** (1981). Properties and distribution of ionic conductances
564 generating electroresponsiveness of mammalian inferior olivary neurons *in vitro*. *J.*
565 *Physiol. (Lond)* **315**, 569-584. <https://doi.org/10.1113/jphysiol.1981.sp013764>
- 566 **Lo, M. V. C. and Shrager, P.** (1981). Block and inactivation of sodium channels in
567 nerve by amino acid derivatives. *Biophys. J.* **35**, 31-43. [doi.org/10.1016/0165-](https://doi.org/10.1016/0165-0270(93)90069-4)
568 [0270\(93\)90069-4](https://doi.org/10.1016/0165-0270(93)90069-4)
- 569 **Loi, P. K. and Tublitz, N. J.** (1997). Molecular analysis of FMRFamide- and
570 FMRFamide-related peptides (FaRPs) in the cuttlefish, *Sepia officinalis*. *J. Exp. Biol.*
571 **200**, 1483-1489.
- 572 **Loi, P. K. and Tublitz, N. J.** (2000). Role of glutamate and FMRFamide-related
573 peptides at the chromatophore neuromuscular junction in the cuttlefish, *Sepia*
574 *officinalis*. *J. Comp. Neurol.* **420**, 499-511. doi: [10.1002/\(SICI\)1096-](https://doi.org/10.1002/(SICI)1096-9861(20000515)420:4<499::AID-CNE7>3.0.CO;2-E)
575 [9861\(20000515\)420:4<499::AID-CNE7>3.0.CO;2-E](https://doi.org/10.1002/(SICI)1096-9861(20000515)420:4<499::AID-CNE7>3.0.CO;2-E)
- 576 **Lucero, M. T. Horrigan, F. T. and Gilly, V. F.** (1992). Electrical responses to
577 chemical stimulation of squid olfactory receptor cells. *J. Exp. Biol.* **162**, 231-249.
578 doi: [10.1098/rstb.2000.0670](https://doi.org/10.1098/rstb.2000.0670)
- 579 **Mitra, R. and Morad, M.** (1986). Two types of calcium channel in guinea pig
580 ventricular myocytes. *Proc. Natl. Acad. Sci. USA* **83**, 5340-5344. doi:
581 [10.1073/pnas.83.14.5340](https://doi.org/10.1073/pnas.83.14.5340)
- 582 **Mues, G., Fuchs, I., Wei, E. T., Weber, E., Evans, C. J., Barchas, J. D. and**
583 **Chang, J. K.** (1982). Blood pressure elevation in rats by peripheral administration of
584 Tyr-Gly-Gly-Phe-Met-Arg-Phe and the invertebrate neuropeptide, Phe-Met-Arg-Phe-
585 NH₂. *Life Sciences* **31**, 2555-2561. doi: [10.1016/0024-3205\(82\)90728-7](https://doi.org/10.1016/0024-3205(82)90728-7)
- 586 **Muthal, A. V., Mandhane, S. N. and Chopode, C. T.** (1997) Central administration
587 of FMRFamide produces antipsychotic-like effects in rodents. *Neuropeptides* **31**, 319-
588 322. doi: [10.1016/s0143-4179\(97\)90065-2](https://doi.org/10.1016/s0143-4179(97)90065-2)
- 589 **Neher, E.** (1971). Two fast transient current components during voltage-clamp on
590 snail neurons. *J. Gen. Physiol.* **58**, 36-53. doi: [10.1085/jgp.58.1.36](https://doi.org/10.1085/jgp.58.1.36)
- 591 **Nelson, L. S., Kim, K., Memmott, J. E. and Li, C.** (1998). FMRFamide-related gene
592 family in the nematode, *Caenorhabditis elegans*. *Mol. Brain Res.* **58**, 102-111. doi:
593 [10.1016/s0169-328x\(98\)00106-5](https://doi.org/10.1016/s0169-328x(98)00106-5)

- 594 **Nishimura, M., Ohtsuka, K., Takahashi, H. and Yoshimura, M.** (2000). Role of
595 FMRFamide-activated brain sodium channel in salt-sensitive hypertension.
596 *Hypertension* **35**, 443-450. doi.org/10.1161/01.HYP.35.1.443
- 597 **Nowycky, M., Fox, A. P. and Tsien, R. W.** (1985). Three types of neuronal calcium
598 channel with different calcium agonist sensitivity. *Nature* **316**, 440-443. doi:
599 [10.1038/316440a0](https://doi.org/10.1038/316440a0)
- 600 **Ödholm, M. P., Williamson, R. and Jones, M. B.** (2000). Ionic currents in cardiac
601 myocytes of squid, *Alloteuthis subulata*. *J. Comp. Physiol. B* **170**:11-20.
602 doi.org/10.1007/s003600050002
- 603 **O'Donohue, T. L., Bishop, J. F., Chronwall, B. M. Groome, J. and Watson, W. H.**
604 (1984). III. Characterization and distribution of FMRF-amide immunoreactivity in the
605 rat central nervous system. *Peptides* **5**, 563-568. doi: [10.1016/0196-9781\(84\)90087-1](https://doi.org/10.1016/0196-9781(84)90087-1)
- 606 **Price, D. A. and Greenberg, M. J.** (1977). Structure of a molluscan cardioexcitatory
607 neuropeptide. *Science* **197**, 670-671. doi: [10.1126/science.877582](https://doi.org/10.1126/science.877582)
- 608 **Price, D. A. and Greenberg, M. J.** (1989). The hunting of the FaRPs: distribution of
609 the FMRFamide-related peptides (FaRPs). *Biol. Bull.* **177**, 198-205. doi:
610 [10.2307/1541933](https://doi.org/10.2307/1541933)
- 611 **Raffa, R. B., Heyman, J. and Porreca, F.** (1986). Intrathecal FMRFamide (Phe-
612 Met-Arg-Phe-NH₂) induces excessive grooming behavior in mice. *Neurosci. Lett.* **65**,
613 94-98. doi: [10.1016/0304-3940\(86\)90126-6](https://doi.org/10.1016/0304-3940(86)90126-6)
- 614 **Raffa, R. B. and Stone, D. J.** (1996). Could dual G-protein coupling explain [D-Met
615 (2)] FMRFamide's mixed action *in vivo*? *Peptides* **17**, 1261-1265.
- 616 **Rémy, C., Guy, J., Pelletier, G. and Boer, H. H.** (1988). Immunohistological
617 demonstration of a substance related to neuropeptide Y and FMRFamide in the
618 cephalic and thoracic nervous systems of locust *Locusta migratoria*. *Cell Tissue Res.*
619 **254**, 189-195. doi [10.1007/BF00220033](https://doi.org/10.1007/BF00220033)
- 620 **Saidel, W. M.** (1979). Relationship between photoreceptor terminations and
621 centrifugal neurons in the optic lobe of octopus, *Cell Tissue Res.* **204**, 463-472. doi:
622 [10.1007/bf00233657](https://doi.org/10.1007/bf00233657)
- 623 **Saito, M. and Wu, C. F.** (1991). Expression of ion channels and mutational effects in
624 giant drosophila neurons differentiated from cell division arrested embryonic

- 625 neuroblasts. *J. Neurosci.* **11(7)**, 2135-2150. doi: [10.1523/JNEUROSCI.11-07-](https://doi.org/10.1523/JNEUROSCI.11-07-02135.1991)
626 [02135.1991](https://doi.org/10.1523/JNEUROSCI.11-07-02135.1991)
- 627 **Sasayama, Y., Katoh, A., Oguro, C., Kambegawa, A. and Yoshizawa, H.** (1991)
628 Cells showing immunoreactivity for calcitonin or calcitonin gene-related peptide
629 (CGRP) in the central nervous system of some invertebrates, *Gen. Comp. Endocrinol.*
630 **83**, 406–414. doi: [10.1016/0016-6480\(91\)90146-w](https://doi.org/10.1016/0016-6480(91)90146-w)
- 631 **Schneider, L. E. and Taghert, P. H.** (1988). Isolation and characterization of a
632 *Drosophila* gene that encodes multiple neuropeptide related to Phe-Met-Arg-Phe-NH₂
633 (FMRFamide). *Proc. Natl. Acad. Sci. USA* **85**, 1993-1997. doi:
634 [10.1073/pnas.85.6.1993](https://doi.org/10.1073/pnas.85.6.1993)
- 635 **Scott, R. H., Pearson, H. A. and Dolphin, A. C.** (1991). Aspects of vertebrate
636 neuronal voltage-activated calcium currents and their regulation. *Prog. Neurobiol.* **36**,
637 485-520. doi: [10.1016/0301-0082\(91\)90014-r](https://doi.org/10.1016/0301-0082(91)90014-r)
- 638 **Sorenson, R. L., Sasek, C. A. and Elde, R.P.** (1984) Phe-Met-Arg-Phe-amide
639 (FMRF-NH₂) inhibits insulin and somatostatin secretion and anti-FMRFA-NH₂ sera
640 detects pancreatic polypeptide cells in rat islet. *Peptides* **5**, 777-782.
641 [https://doi.org/10.1016/0196-9781\(84\)90021-4](https://doi.org/10.1016/0196-9781(84)90021-4)
- 642 **Suzuki, H., Yamamoto, T., Inenaga, M. and Uemura, H.** (2000). Galanin-
643 immunoreactive neuronal system and localization with serotonin in the optic lobe and
644 peduncle complex of the octopus (*Octopus vulgaris*), *Brain Res.* **865**, 168–176. doi:
645 [10.1016/s0006-8993\(00\)02191-0](https://doi.org/10.1016/s0006-8993(00)02191-0)
- 646 **Suzuki, H., Yamamoto, T., Nakagawa, M. and Uemura, H.** (2002). Neuropeptide
647 Y-immunoreactive neuronal system and colocalization with FMRFamide in the optic
648 lobe and peduncle complex of octopus (*Octopus vulgaris*). *Cell. Tissue Res.* **307**, 255-
649 264. doi: [10.1007/s00441-001-0492-9](https://doi.org/10.1007/s00441-001-0492-9)
- 650 **Tasaki, I. and Hagiwara, S.** (1957). Demonstration of two stable potential states in
651 the squid giant axon under tetraethylammonium chloride. *J. Gen. Physiol.* **40**, 859-
652 885. doi: [10.1085/jgp.40.6.859](https://doi.org/10.1085/jgp.40.6.859)
- 653 **Tasaki, K., Tsukahara, Y., Suzuki, H. and Nakaye, T.** (1982). Two types of
654 inhibition in the cephalopod retina. In Kaneko A, Tsukahara N, Uchizono K (eds)
655 Neurotransmitters in the Retina and the Visual Centers. Biomedical Res. Suppl,
656 Tokyo pp 41-44.

- 657 **Thiemermann, C., Al-Damluji, S., Hecker, M. and Vane, J. R.** (1991). FMRF-
658 amide and L-Arg-l-Phe increase blood pressure and heart rate in the anaesthetized rat
659 by central stimulation of the sympathetic nervous system. *Biochem. Biophys. Res.*
660 *Commun.* **175**, 318-324. doi: [10.1016/s0006-291x\(05\)81237-9](https://doi.org/10.1016/s0006-291x(05)81237-9)
- 661 **Thompson, S. H.** (1977). Three pharmacologically distinct potassium channels in
662 molluscan neurons. *J. Physiol. (Lond)* **265**, 465-488. doi:
663 [10.1113/jphysiol.1977.sp011725](https://doi.org/10.1113/jphysiol.1977.sp011725)
- 664 **Walker, R. J., Papaioannou, S. and Holden-Dye, L.** (2009). A review of
665 FMRFamide and RFamide-like peptides in metazoa. *Invertebr. Neurosci.* **9**, 111–153.
666 doi: [10.1007/s10158-010-0097-7](https://doi.org/10.1007/s10158-010-0097-7)
- 667 **Wang, X., McKenzie, J. S. and Kemm, R. E.** (1996) Whole cell calcium currents in
668 acutely isolated olfactory bulb output neurons of the rat. *J. Neurophysiol.* **75**, 1138-
669 1151. doi: [10.1007/s10158-010-0097-7](https://doi.org/10.1007/s10158-010-0097-7)
- 670 **Wang, X. Y., Morishita, F., Matsushim, O. and Fujimoto, M.** (2000). Carassius
671 RFamide, a novel FMRFa-related peptide, is produced within the retina and involved
672 in retinal information processing in cyprinid fish. *Neurosci. Lett.* **289**, 115-118. doi:
673 [10.1016/s0304-3940\(00\)01281-7](https://doi.org/10.1016/s0304-3940(00)01281-7)
- 674 **Williamson, R. and Chrachri, A.** (2004). Cephalopod Neural Networks
675 *Neurosignals* **13**, 87-98. doi: [10.1159/000076160](https://doi.org/10.1159/000076160)
- 676 **Wu, J. and Lipsius, S. L.** (1990). Effects of extracellular Mg²⁺ on T- and L-type Ca²⁺
677 currents in single atrial myocytes. *Am. J. Physiol.* **259**, H1842-H1850.
678 doi.org/[10.1152/ajpheart.1990.259.6.H1842](https://doi.org/10.1152/ajpheart.1990.259.6.H1842)
- 679 **Yakel, J. L.** (1991). The neuropeptide FMRFamide both inhibits and enhances the
680 Ca²⁺ current in dissociated *Helix* neurones via independent mechanisms. *J.*
681 *Neurophysiol.* **65**, 1517-1527. doi.org/[10.1152/jn.1991.65.6.1517](https://doi.org/10.1152/jn.1991.65.6.1517)
- 682 **Yamamoto, T., Tasaki, K., Sugawara, Y. and Tonosaki, A.** (1965). Fine structure
683 of octopus retina. *J. Cell. Biol.* **25**, 345-359. doi: [10.1083/jcb.25.2.345](https://doi.org/10.1083/jcb.25.2.345)
- 684 **Yamamoto, M. and Takasu, N.** (1984). Membrane-particles and gap-junctions in the
685 retinas of 2 species of cephalopods, *Octopus ocellatus* and *Sepiolla japonica*. *Cell*
686 *Tissue Res.* **237** (2), 209-218. doi: [10.1007/BF00217138](https://doi.org/10.1007/BF00217138)
- 687 **Young, J. Z.** (1962). The optic lobe of *Octopus vulgaris*, *Philos. Trans. R. Soc. B*
688 *Biol. Sci.*, **245**, 19–58. doi.org/[10.1098/rstb.1962.0004](https://doi.org/10.1098/rstb.1962.0004)

- 689 **Young, J. Z.** (1971). The anatomy of the nervous system of *Octopus vulgaris*.
690 Clarendon, Oxford. doi: [10.3389/fphys.2019.01637](https://doi.org/10.3389/fphys.2019.01637)
- 691 **Young, J. Z.** (1974). The central nervous system of *Loligo*. I. The optic lobe. *Phil.*
692 *Trans. R. Soc. B Lond.* **267**, 263-302. doi.org/[10.1098/rstb.1974.0002](https://doi.org/10.1098/rstb.1974.0002)
- 693 **Zhu, Y., Sun, L.L., Wu, J.H., Liu, H., Zheng, L., Lü, Z. and Chi, C.** (2020). An
694 FMRFamide Neuropeptide in Cuttlefish *Sepia pharaonis*: Identification,
695 Characterization, and Potential Function. *Molecules* (Basel, Switzerland). Apr; 25(7).
696 doi: [10.3390/molecules25071636](https://doi.org/10.3390/molecules25071636)
- 697

698 **Figure legends**

699 **Fig. 1 Morphology and overall ionic currents recorded from an identified**
700 **centrifugal neuron in the optic lobe of cuttlefish. A)** Lucifer yellow-filled
701 centrifugal neuron with the characteristic numerous fine branches in the plexiform
702 zone (*arrow heads*). o.gr.: outer granule cell layer, pl: plexiform zone and i.gr.: inner
703 granule cell layer. **B)** An evoked antidromic action current resulting from stimulation
704 of the appropriate optic nerve bundle. **C)** Whole-cell currents recorded from a
705 centrifugal neuron. Overall response to a series of voltage steps (with 20 mV
706 increments) from a holding potential of -60 mV is composed of an outward current
707 (*open circle*), a transient inward current (*filled circle*) and a smaller inward current
708 (*filled triangle*). **D)** *I-V* plots of the outward current (*open circles*) and an inward
709 current (*filled circles*). Horizontal bar: 50 μm (**A**).

710

711 **Fig. 2 Voltage and pharmacological separation of A-current in an identified**
712 **centrifugal neuron. A)** Whole cell outward current in response to membrane
713 depolarization to voltage steps from a holding potential of -60 mV. Total outward
714 current is composed of a transient outward current and a sustained outward current. **B)**
715 Whole cell outward current in response to membrane depolarization to the same
716 voltage steps as in **A** but this time from a holding potential of -40 mV. The A-current
717 is largely inactivated at this holding potential, leaving only the sustained outward
718 current or delayed rectifier (I_K). **C)** Computer subtraction of **B** and **A** to show the
719 isolated transient outward current or A-current (I_A). **D)** *I-V* plots of the instantaneous
720 currents 5 ms after the start of the voltage steps for the total outward current (*circles*),
721 the mainly I_K current (*squares*) and the isolated I_A (*triangles*). **E)** Whole cell outward
722 current in response to membrane depolarization to a voltage step of +50 mV from a
723 holding potential of -80 mV. Total outward current is composed of a transient outward
724 current and a sustained outward current (control). Bath application of 4 mM 4-AP
725 suppressed the transient outward current, leaving only the sustained outward current
726 (4-AP). Bath application of TEA suppressed 75% of this sustained outward current. **F)**
727 *I-V* plots of the instantaneous currents 5 ms after the start of the voltage steps for the
728 total outward current (*open circles*), the mainly I_K current (*filled circles*) and after the
729 application of TEA (*filled triangles*).

730

731 **Fig. 3 Inward currents recorded from an identified centrifugal neuron. A)** In the
732 control, the whole-cell currents from this cell obtained in response to a series of
733 voltage steps (*bottom*), from a holding potential of -60 mV. **B)** 5 minutes after bath
734 application of an ASW containing TTX (1 μ M), the Na⁺ current disappeared leaving
735 only a sustained inward current. **C)** TTX-sensitive current in isolation, which is
736 obtained by computer subtraction of **B** from **A**.

737

738 **Fig. 4 Identification of the L-type calcium current. A)** Effect of barium chloride on
739 the sustained inward current, whole cell inward current in a centrifugal neuron in
740 response to a voltage step to 0 mV from a holding potential of -60 mV before
741 (*control*) and after (*BaCl₂*) substitution of barium for calcium in the external solution
742 which resulted in an increase in the amplitude of the calcium current. **B)** Effect of
743 cobalt chloride at a concentration of 4 mmol l⁻¹ on the sustained inward current, whole
744 cell inward current in a centrifugal neuron in response to a voltage step to -10 mV
745 from a holding potential of -60 mV before (*control*) and after (*CoCl₂*) was added into
746 the external solution resulted in total blockade of the calcium current. **C)** Similarly,
747 nifedipine (5 μ mol l⁻¹) also suppressed completely this sustained calcium current. **D)**
748 Representative example of membrane currents during a test-pulse to -30 mV from a
749 holding voltage of -80 mV (a) or -60 mV (b); the difference current (a-b) is the T-type
750 Ca²⁺ current. **E)** Peak current-voltage (I/V) relation of the same centrifugal neuron.
751 For this I/V plot current traces are displayed, when the holding potential was -80 mV
752 (*open circles*), when the holding potential was -60 mV (*filled circles*), and finally the
753 difference current (*triangles*).

754

755 **Fig. 5 FMRamide inhibits both the I_A and I_K in centrifugal neuron. A)** Current
756 traces recorded in response to membrane depolarization to a voltage step of -60, -20,
757 +20, +50, +60 and +70 mV from a holding potential of -60 mV prior to the
758 application of FMRFa. **B)** Reduction of K⁺ currents by FMRFa (1 μ M). **C)** Recovery
759 of K⁺ currents after FMRFa had been washed out. **D)** Difference current obtained by
760 subtracting current profiles obtained in the presence of FMRFa (**B**) from those
761 obtained before the application of FMRFa (**A**) demonstrates that FMRFa blocked both

762 the fast transient component, I_A (*arrow head*), as well as the sustained and slowly
763 inactivating potassium current, I_K (*doubled arrow head*).

764

765 **Fig. 6 FMRFamide-mediated inhibition of I_{Na} and $I_{Ca,L}$ in a centrifugal neuron.**

766 **A)** Current traces recorded in response to membrane depolarization to a voltage step
767 of -10 mV from a holding potential of -60 mV before (*control*) and after (*FMRFa*)
768 bath application of 1 μ M FMRFa, first after 5 minutes (*grey trace*) and then 8 minutes
769 (*dark trace*). These currents trace not only show that FMRFa inhibited I_{Na} (*star*), but
770 also $I_{Ca,L}$ (*triangle*). **B)** I-V relationship of I_{Na} before (*open circles*), 5 minutes and then
771 8 minutes after (*grey and filled circles*, respectively).

772

773 **Fig. 7 Effect of FMRFamide on calcium currents in centrifugal neuron. A)** Left

774 traces are current traces recorded in response to membrane depolarization to a voltage
775 step of -40 mV from a holding potential of -80 mV showing that FMRFa had no
776 apparent effect on the transient component of the calcium current. Right traces are
777 current recorded in response to membrane depolarization of the same centrifugal
778 neuron to a voltage step of 0 mV from a holding potential of -80 mV before (*black*
779 *trace*) and after (*grey trace*) the application of FMRFa demonstrating that this
780 neuropeptide decrease the amplitude of the $I_{Ca,L}$. **B)** I-V relationship of both calcium
781 current under control conditions (*black circles*), and after the application of FMRFa
782 (*grey circles*). **C)** Time course of the onset, and recovery from, the effect of
783 FMRFamide on $I_{Ca,L}$.

784

785

786

787

788

Figures

Fig. 1

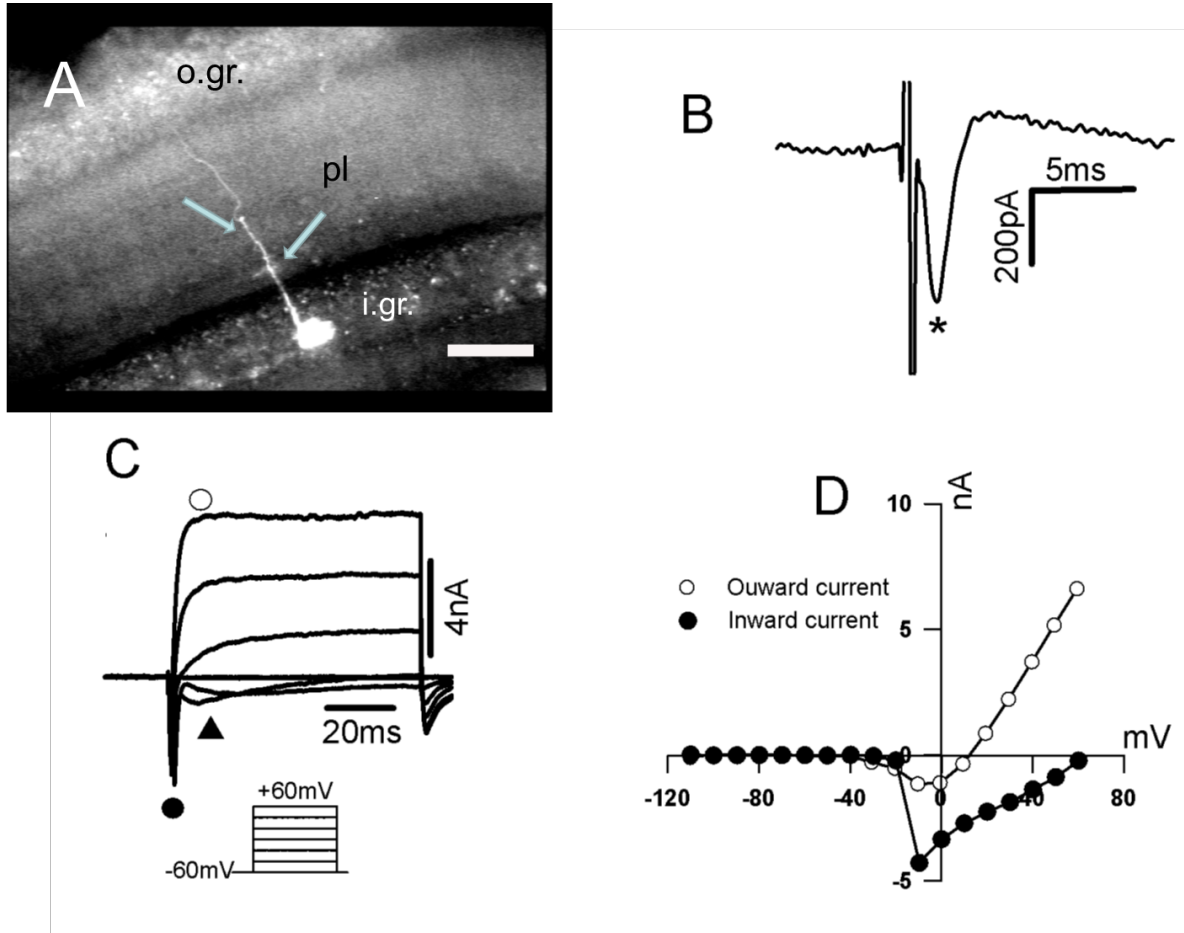


Fig.2

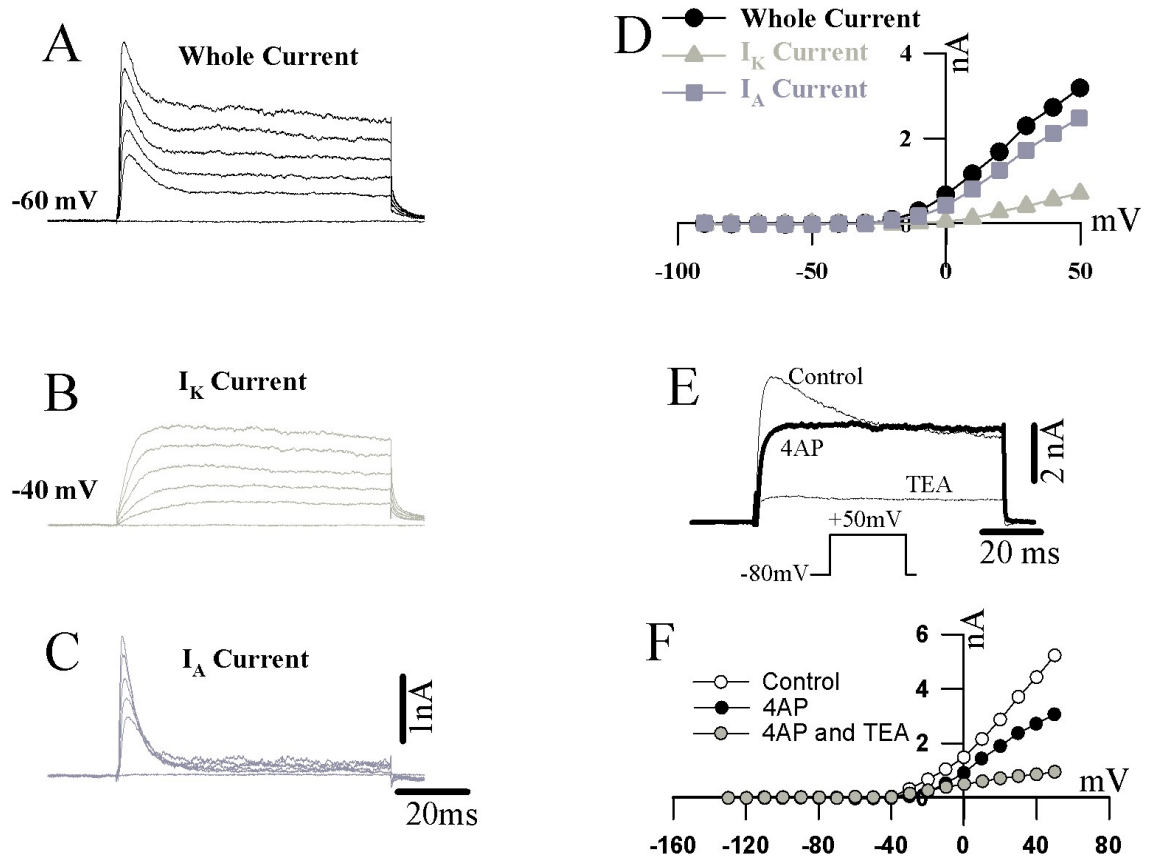


Fig.3

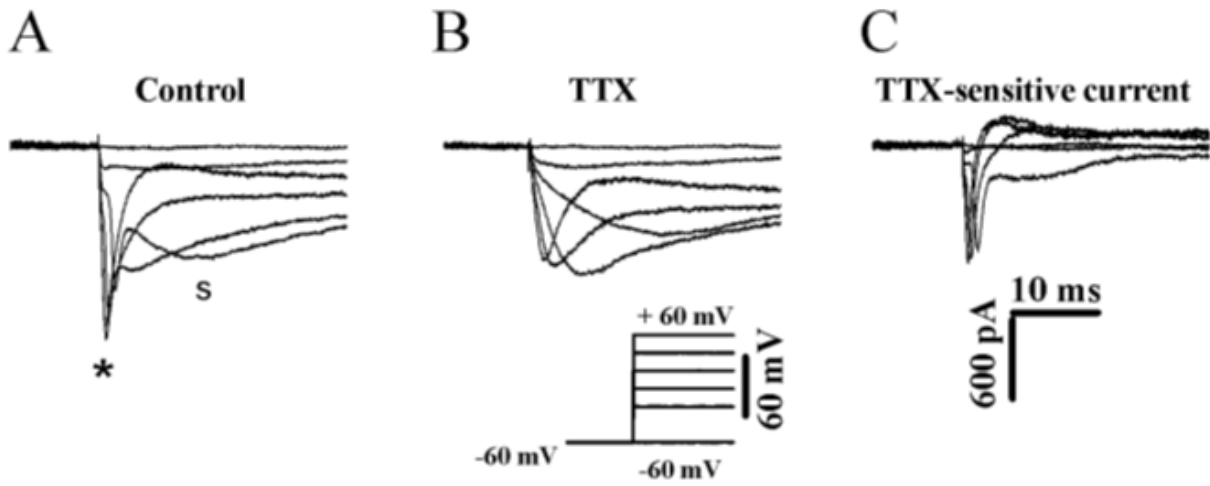


Fig.4

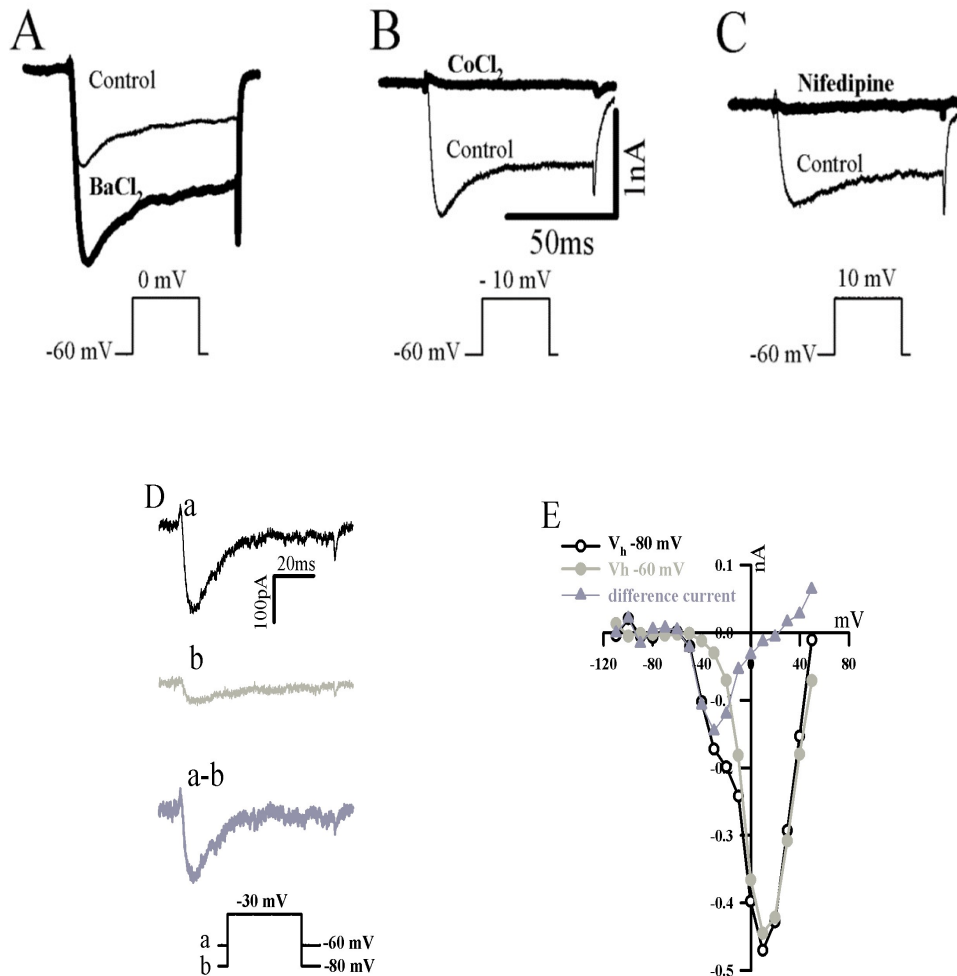


Fig.5

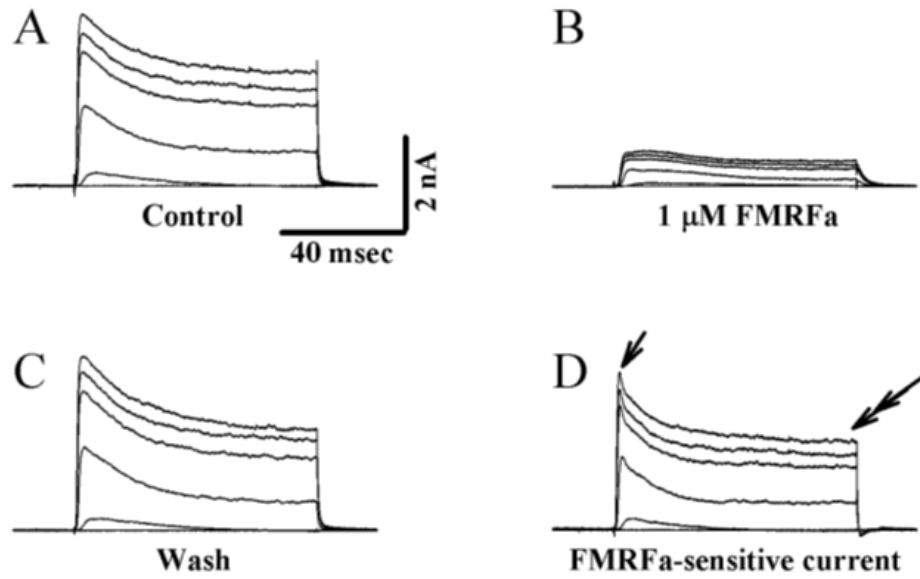


Fig.6

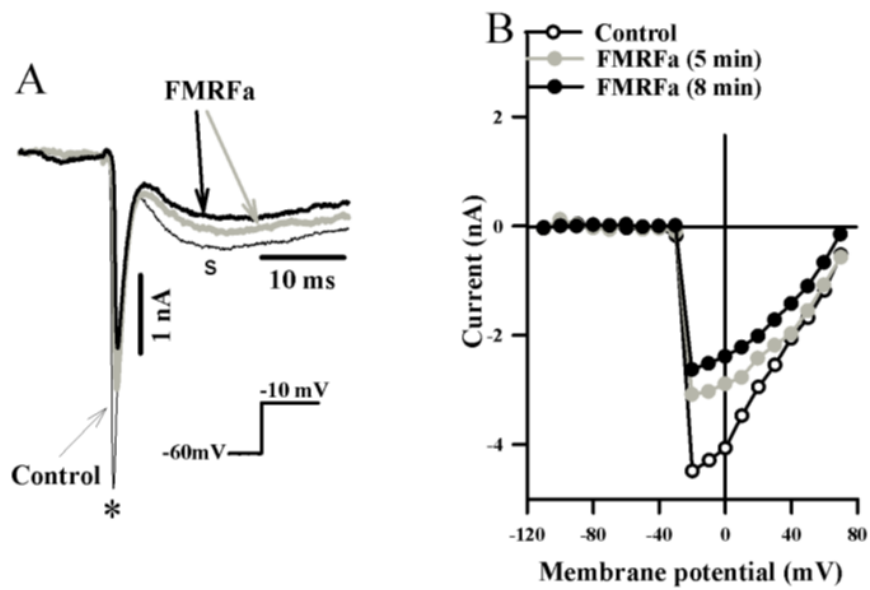


Fig.7

